FREE for Reading & Publication
Diamond Open Access

Resonance-Based Temperature Sensors using a Wafer Level Vacuum Packaged SOI MEMS Process

Gulsah Demirhan Aydin[1,*], Tayfun Akin[1,2]

[1]METU MEMS Centre, Middle East Technical University, Ankara, 06510, Turkey
[2]Electrical and Electronics Eng. Department, Middle East Technical University, Ankara, 06800, Turkey

***Corresponding author: E-mail: gdemirhan@mems.metu.edu.tr; Tel.: (+90) 312 210 6377**

DOI: 10.5185/amlett.2020.011462

This paper reports the development of resonance-based temperature sensors using a wafer level vacuum packaged SOI MEMS process which is normally used to implement various MEMS sensors, including MEMS gyroscopes and accelerometers. Implementing MEMS temperature sensors in such a MEMS process together with sensitive MEMS sensors allows obtaining temperature data, which is very useful for the compensation of a number of parameters of these MEMS sensors for obtaining improved performance from these sensors. Four different types of temperature sensors are designed considering two types of actuation mechanisms (varying gap and varying overlap) and two different mass types (H-shaped single mass and tuning fork double mass), and their design and model analysis are verified using finite element modelling (FEM) simulations. All of the sensors are fabricated in the same die by using the advanced MEMS (aMEMS) process [1]. The fabricated sensors are combined with necessary readout electronics for each structure in LT Spice environment, and their proper operations are verified in MATLAB Simulink. The temperature sensing technique is based on the frequency variations due to the thermal expansion coefficient mismatch between the glass substrate and the silicon that causes a mechanical strain on the resonator and to a smaller extent, by the temperature variation of Si Young modulus, which influences the resonance frequency. The performance of each sensor is measured using the real time data acquisition from the resonators where resonance frequency and resonator controller outputs are monitored for different temperatures. The best performance is obtained with the tuning fork double mass together with varying gap structures, where the temperature coefficient of frequency (TCF) values are measured as -128 ppm/K in the measurement range in the hot plate and as -114 ppm/K in the measurement range in the oven.

Introduction

Micro-Electro-Mechanical Systems (MEMS) is the synergistic integration of mechanical and electrical components. In recent years, various MEMS products including inertial sensors, flow and pressure sensors, RF MEMS, optical MEMS, power MEMS, and BioMEMS are replaced their macro scale counter parts in the market. Micro-Electro-Mechanical Systems (MEMS) having capacitive sensing mechanism, which is the branch of inertial sensors, have been gaining interest as a result of low-cost, small-size, and high- reliability sensors applications [**2**,**3**]. Today micro-machined sensors can be found in different places and various areas ranging from military to industrial applications such as inertial navigation, vibration monitoring, and robotics control.

MEMS resonators are the type of physical sensors which can be utilized in combination with many other MEMS sensors. The wide-variety of use of MEMS resonators has made these devices an attraction point to the researchers to focus on. The utilities of MEMS resonators both in industrial and research-based applications are resulted with different types of MEMS resonators such as ring resonators, contour/lame mode plate resonators, bulk acoustic wave resonators in different applications including the optical, photonic and acoustic systems [**4–8**].

MEMS resonators are used in electronic oscillators that generate an electrical signal at the resonance frequency and a significant issue for MEMS oscillators is their stability with changes in the ambient temperature. Another common use of MEMS resonant-based sensor is the timing and frequency reference applications instead of quartz crystals [**9**]. The removal of the inherent temperature dependence of silicon- based MEMS resonators is a hot topic for the reference application purposes. While many studies have focused on this issue, [**10–14**] temperature dependency of the MEMS resonators brings up the temperature sensor adoption of MEMS resonators.

There are mainly two methods for achieving thermal compensation of a MEMS structures named by hardware circuit design or by processing the data, after reading from a sensor output. In comparison, hardware compensation is faster than the processing of the data. On the other hand, in some cases it is impossible to use the hardware

compensation and the signal processing is the only available option due to the lack of many design considerations and the internal characteristics of the sensor. Temperature compensation by hardware design options in the literature can be listed as: using temperature control device; controlling the oscillators using PTAT (Proportional to Absolute Temperature); using temperature variable gain circuit; design targeting temperature compensation; and using frequency synthesizer for core temperature. In this particular study, only temperature compensations by signal processing is selected and the real-time temperature compensation will not be intended. Temperature compensation by signal processing options in the literature can be similarly listed as: applying Kalman filter method; applying moving average filter method; applying wavelet decomposition; applying polynomial curve fitting; applying linear curves; applying back propagation neural networks; and applying temperature coefficient of resonant frequency.

MEMS based sensors do also have some drawbacks that restrict them to be used in applications that require inertial grade accuracy. MEMS devices, in terms of resonating structures, require mechanical movement for the operation and material is heated causing changes in the output of a sensor. For instance, an accelerometer's output gives a measurement in terms of "g"; and one of the most significant disadvantages of its output is the drift in the g output of the chip.

Therefore, the objective of this research is to introduce the development of resonance-based temperature sensors using a wafer level vacuum packaged SOI MEMS process for temperature compensation of MEMS gyroscopes and accelerometers.

This paper reports the design, fabrication, test and comparison of different types of hermetically encapsulated resonance-based MEMS temperature sensors. The idea is to employ the resonator structure as a temperature sensor together with a controller circuitry. In the scope of this study, mainly two different types of micro-resonators are designed; single-mass H-shaped resonators and tuning fork (double mass) resonators to obtain a high-quality factor resonating structures. The verification of modal analysis is carried out in finite element modelling (FEM) simulations of the micromachined resonators. In order to make an exact comparison in the same environmental conditions, the single mass and tuning fork type, totally 4 different resonator designs are implemented in the same die. Wafer level hermetic packaging of the resonating structure is performed at the end of the process of the sensor substrate and silicon on insulator (SOI) cap substrate with anodic bonding technique. The readout electronics for micromechanical resonators are proposed with schematics and the simulations in freeware computer software; and then, the MEMS sensor and front-end electronics is integrated on a hybrid glass substrate after convenient design and fabrication. Then, the integration of the resonator sensors and glass substrate's real time data acquisition from the resonator as temperature sensor is achieved on resonance frequency and resonator controller outputs by using both hot plate and temperature oven with checking hysteresis, too. The resonator sensor designs characterized separately, and their temperature dependencies are investigated. It is found that there is a relation between the changing temperature and resonator's resonance frequency and also resonator's controller output. The temperature look- up graphs are created to express the temperature by the means of resonator's PI controller output voltage. This relation is given to allow for calculation of the temperature for the associated controller output voltage. It is found that tuning fork types show better performance compared to single mass ones. Therefore, tuning fork varying gap design of resonator structures can be used to provide input to the studies to be carried out to eliminate the temperature change of sensors as they can preclude the need for heating or electronic compensation, allowing for lower power compensation and better phase noise performance due to the reduced complexity of the control electronics.

Experimental

A. Resonator design and modeling

It is aimed to use the designed resonator structure as a temperature sensor together with controller circuitry, which is the main reason for designing two types of resonators. First one is, single-mass H-shaped resonator with two different actuation mechanisms called varying gap and varying overlap with resonance frequency of 15 kHz. The other one is tuning fork (double mass) resonator. By selecting a tuning fork (TF) structure, it is expected to obtain a high quality factor resonating structure. Similarly, in this type, there will be two different actuation mechanism types called varying gap and varying overlap and each of these with resonance frequency of 15 kHz.

The different actuation mechanisms are selected to make a comparison between the performances. For instance, varying overlap area type capacitors are used for a large displacement whereas varying gap type capacitors are used to get higher capacitive sensitivity which is required to detect small displacements. However, in the varying gap type actuation mechanism, the main challenge is the non-linear behavior. Similarly, the different mass types are selected because of performance comparison purposes. Obviously, single proof mass has a natural advantage of fabrication and size reduction whereas conventional single resonant sensor has such advantages, it has also some drawbacks ranging from lower sensitivity to more sensitivity to ambient changes.

Therefore, in this study there will be totally 4 different types of designs; and for each 4 type the analytical derivations are performed by hand calculations. In analytical derivations Young's modulus, resonance frequency, quality factor, expansion of materials, spring, mass and damping factor estimation and electrostatic actuation (varying gap or varying overlap type), number of capacitive fingers, finger thickness, width and gap,

capacitance and derivative of capacitance with respect to displacement are considered as design parameters. **Table 1** presents the geometrical properties and the design parameters of the resonator structures for all designs.

Table 1. The geometrical properties and the design parameters of the resonator systems.

Parameters	Design-1	Design-2	Design-3	Design-4
# of capacitive fingers (N)	77	24	98	48
Finger overlap length (l)	20 µm	95 µm	20 µm	95 µm
Finger width (w)	4 µm	4 µm	4 µm	4 µm
Finger gap (d)	2 µm	2 µm	2 µm	2 µm
Finger anti-gap ($d_{anti-gap}$)	-	6 µm	-	6 µm
Finger thickness (t)	35 µm	35 µm	35 µm	35 µm
Capacitance (C) (Gap)	4.8 pF	3.5 pF	6.1 pF	7.1 pF
dC/dx(Gap)	2.39×10^{-8} F/m	1.77×10^{-7} F/m	3.04×10^{-8} F/m	3.53×10^{-7} F/m
Capacitance (C) (Anti-gap)	-	1.1 pF	-	2.4 pF
dC/dx(Anti-gap)	-	1.96×10^{-8} F/m	-	3.92×10^{-8} F/m
Spring Constant (k)	189 N/m	189 N/m	389 N/m	389 N/m
Mass (m)	1.311×10^{-9} kg	1.311×10^{-9} kg	3.970×10^{-8} kg	4.03×10^{-8} kg
Resonance Frequency (f_r)	18 kHz	18 kHz	15 kHz	15 kHz

To obtain resonance frequency values, firstly analytical hand calculations will be performed continuing the resonator designs in L-Edit CAD Software. After that finite-element modelling (FEM) simulations will be conducted to see the mode shapes and modal frequencies of the designed MEMS resonators. **Fig. 1** shows the conducted FEM simulations and comparison results for simulation, hand calculation and measurement for the proposed designs.

B. Sensor fabrication

After verification with finite element modelling, the proposed resonators are fabricated based on MEMS processing procedures. The resonator mask set is designed using the L-Edit Software. In order to make an exact comparison in the same environmental conditions, 4 different resonator designs are implemented in a same die.

SOI cap wafers are preferred for the wafer level hermetic encapsulation of the fabricated sensor wafers. In the cap wafer process 300 µm handle, 2 µm buried oxide and 100 µm device layer thick SOI wafer is used. At the beginning of the cap wafer fabrication, first of all, via openings are patterned on the handle layer of SOI cap wafer. After via openings are formed, vertical feed through and sealing walls are simultaneously constructed on the device layer of the wafer. It should be noticed that these designs would be compatible with both anodic and eutectic bonding. Also, the detailed process and sensor fabrication steps can be found in [**1**].

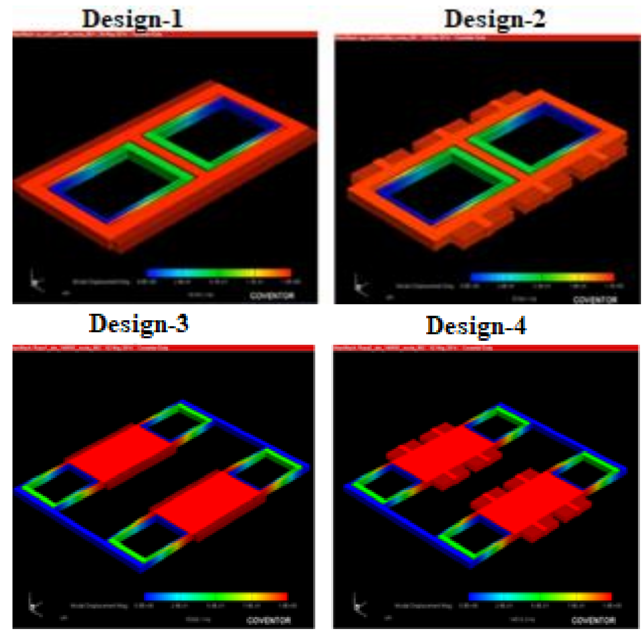

Fig. 1. The conducted FEM simulations and comparison results for simulation, hand calculation and measurement for the TF and single mass varying overlap and varying gap type resonators.

Fig. 2 shows the packaged layout of a die including TF and single mass varying overlap and varying gap type resonators and The SEM picture of the fabricated sensors.

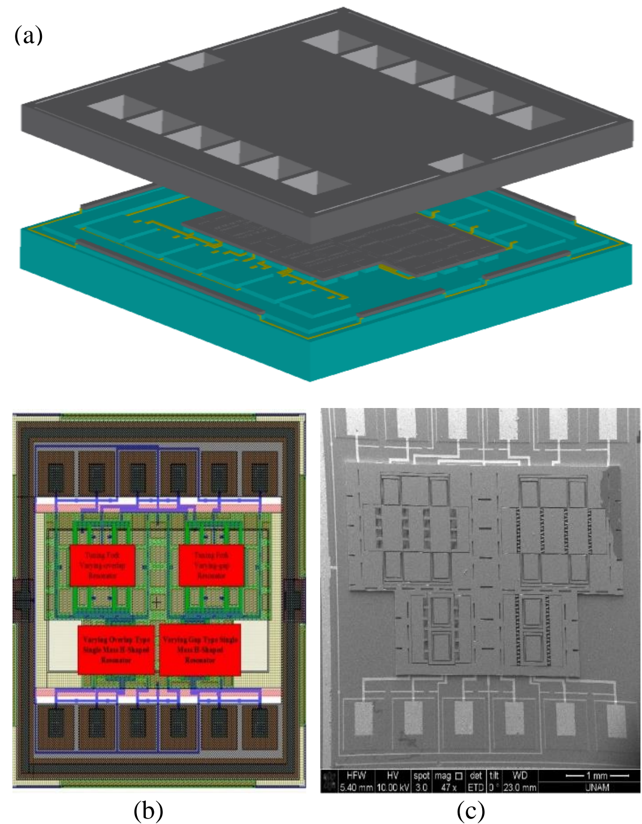

Fig. 2. (a) The resonator mask set is designed by using the L-Edit Software, (b) The packaged layout of a die including TF and single mass varying overlap and varying gap type resonators, (c) The SEM picture of the fabricated sensors.

C. *Readout electronics design*

The operation of the resonator circuitry is relied on an amplitude controlled positive feedback mechanism. Notice that the quality factor of the resonator able to reach to a few tens of thousands in vacuum; therefore, it easily enters the self-oscillation by locking its resonance frequency with the aid of the positive feedback mechanism. After that, with the help of the amplitude control mechanism, the amplitude of the resonator oscillation is set to a certain level.

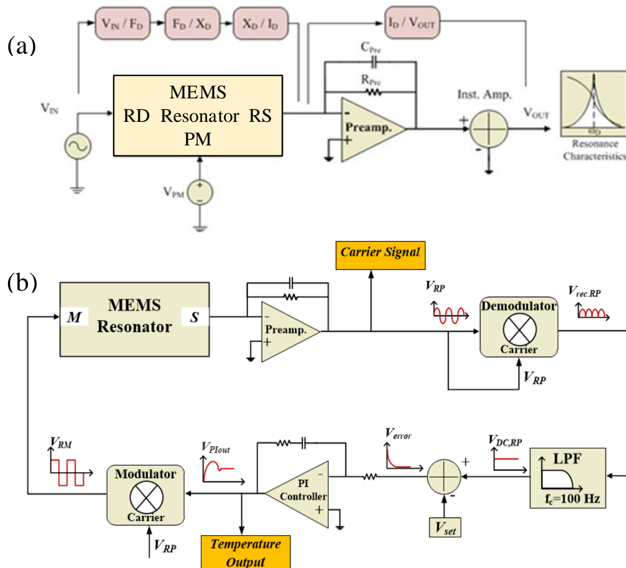

Fig. 3. (a) The simplified block diagram of the resonance test schematic. (b) The scheme representing the block diagram of the closed loop resonator controller circuitry.

In this system, before designing the closed-loop drive mode controller, open-loop characteristic of the MEMS resonator were analyzed with resonance tests in order to obtain the sensor parameters such as the resonance frequency, quality factor, and gain. The **Fig. 3 (a)** gives the simplified block diagram of the resonator test schematic. In the closed-loop system, first of all, the signal is collected from the output of the preamplifier and demodulated by again itself. A resistive type preamplifier is preferred in the system for minimizing the phase error coming from the modulator and demodulator. The output of the demodulator goes through a second-order low pass filter to obtain the DC part of the demodulator signal which presents information about the level of the resonator displacement. The output of the low pass filter is compared with a reference DC voltage to adjust the amplitude of the resonator displacement. In this step, a band gap reference is used as the reference voltage because the output of the band gap reference is quite insensitive to environmental variations. This way, the resonator oscillation is kept constant over time. Then, the error signal is fed to a PI controller which stabilizes the circuit by diminishing the error signal. The DC output of the PI controller is modulated with the motor sense signal. The modulated motor signal is a square wave because of the switching type modulator. Since the system is a high-Q system in vacuum, it behaves like a sharp band-pass filter. Thus, all other harmonics except the first harmonic of the square wave is rejected by the circuitry. As a result, the amplitude controlled self-oscillation is achieved at the resonance frequency. The **Fig. 3(b)** summarizes what described in the above. The detailed information about readout electronics for MEMS resonator sensors could be found in [**15**].

The fabricated sensors are combined with the necessary readout electronics for each structure in LT Spice environment, and their proper operations are verified in MATLAB Simulink. All the passive components and integrated circuits (ICs) constructing resonator readout circuitry are combined with a 16-pin dual in line (DIL) metal package by Schott Corporation with its silver cap which is used as Faraday Cage. The components are mounted on the glass substrate with solder paste as the glue between the gold lines and the component legs by using pick and place machine. After placing the resonator chip to the glass substrate by silver epoxy, some additional electrical connections of the components placed on the glass substrate are achieved through the wire-bonds (**Fig. 4**).

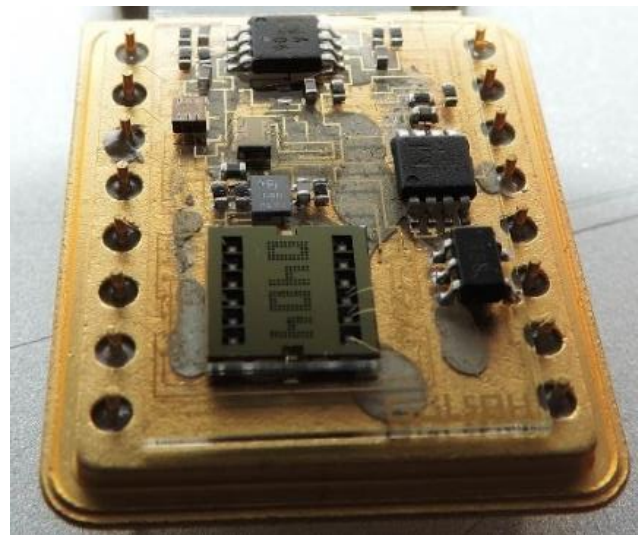

Fig. 4. The image of the fabricated glass substrate together with its entire components attached to 16-pin package.

It is crucial for resonance-based temperature sensor to be satisfied by blocks in the design circuit, which are: preamplifier, gain stage, demodulator, low pass filter, modulator and temperature sensor are analyzed and functionalities are checked. This test is crucial for design of controller electronics for MEMS resonators for the further use of temperature compensation issues.

D. *Implementation and measurement*

The implemented resonator will be shown to satisfy the estimated performance parameters with measurements conducted using various test setups such as functionality tests, resonance tests (to control design is match fabrication or not), temperature tests (to characterize resonator sensor with look up table), C-V tests etc.

Implemented resonator will be applied to resonance tests in open-loop characteristics (to control design is match fabrication or not). Resonance tests indicate resonator sensor characteristics in terms of the natural resonance frequency, quality factor, gain and resonator controller values. Then, open loop temperature tests will be performed to implemented resonator sensor (**Fig. 5**).

The temperature testing will be applied different days and hours (morning to noon) with the same conditions to show the repeatability. The data sampling for the proposed resonators will be applied in the temperature range of room temperature to 90°C for hot plate and -25°C to 120°C for temperature oven (to characterize resonator with look up table).

Implemented resonator will be tested in closed loop temperature versus controller output tests with front end electronics (to characterize resonator sensor with look up table). The temperature testing will be applied different days and hours (morning to noon) with the same conditions to show the repeatability.

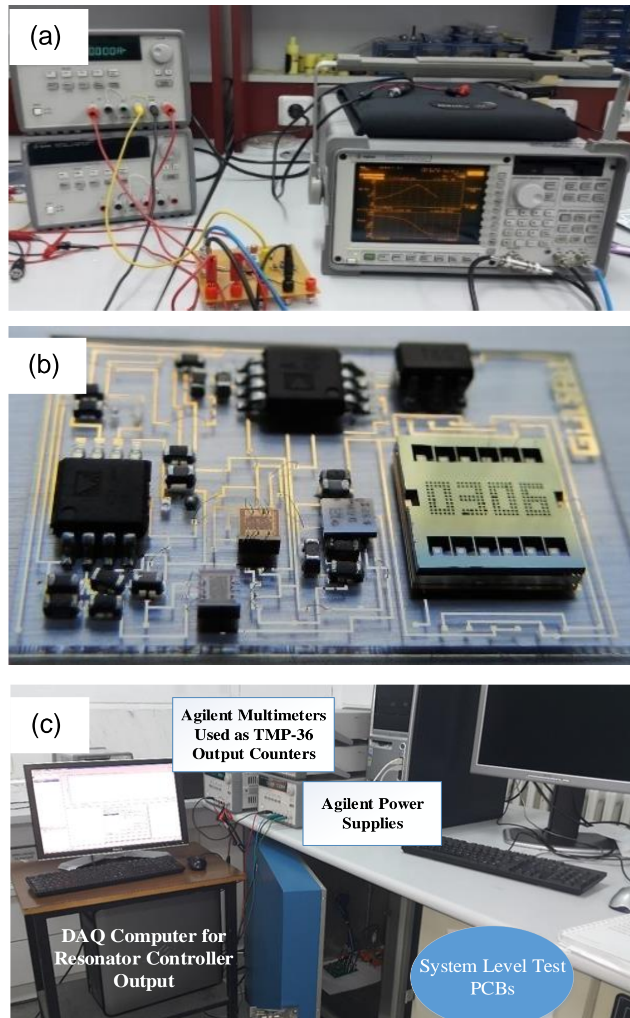

Fig. 5. (a) The image representing resonance test setup, (b) The image of one of the fabricated glass substrates with all the components attached on it and, (c) The Tenney oven in which the system level tests are conducted with data acquisition interface and control module for controlling the test conditions.

After the wire bonding of the packages are completed, tests of the package with front end electronics at different temperatures are started from 20°C to 90°C with 10°C increments. Hot plate is used for temperature settings and to settle the temperature to its exact value duration is nearly 20 minutes. The package is directly put on the hot plate and with the help of wires the connections through the breadboard is constructed. So, the position of the package is never changed or moved. In experiments one of the probes is for ground, one is for the proof mass voltage, one is for resonator sense pad and similarly one other is for resonator drive pad. The preamplifier values obtained in the open-loop characteristics for the resonance tests are used. Notice that the simplified block diagram of the resonance test schematic has already shown in Fig. 3a. **Table 2** shows the result of the best performance resonator sensor (the tuning fork double mass together with varying gap structures) on hot plate. The quality factor values in the tables are calculated as the resonance frequency value in exact temperature over the differences of the 3 dB points for both right-hand side and left-hand side. Also, gain is the output over input in terms of the decibel. After the calculation according to the Equation (**1**) the average TCF value is calculated as -85ppm/°K.

$$f = f0 + f0 * TCF * \Delta T \quad (1)$$

Table 2. Tabulated form of the resonance test results of best performance resonator sensor (the tuning fork double mass together with varying gap structures) is measured using the real time data acquisition from the resonators where resonance frequency is monitored for different temperatures using hot plate. (Notice tests are constructed at 5Hz span, 1mV peak voltage and 5 second of integration and settling time).

Temp. (°C)	Res. Freq. (kHz)	Gain (dB)	Q_R
20	12.874	35.4	114,432
30	12.871	35.1	104,636
40	12.860	33.7	257,198
50	12.849	33.3	171,332
60	12.836	34.4	114,101
70	12.824	34.2	146,555
80	12.808	33.9	102,464
90	12.795	33.2	127,958

Alternatively, instead of bread board after completing the preparation of the test circuitry, tests of the resonator with its preamplifier at the range -25°C to 120°C is done at a temperature chamber which is named Tenney Temperature Oven. For the testing procedure, first of all, related with designed and fabricated resonator packages conventional readout circuitry is placed inside the Tenney oven; and the wires which contain the data come out of the hole which is placed left side of the oven and these wires are connected to the computers and power supplies as shown in the **Fig. 6**.

Although the chamber is able to produce the temperature range from -80°C to 150°C for tests -25°C to 120°C range is preferred. While the oven is turned on the vibration problem is faced which causes a lot of noise while collecting the data. For those reasons different type of testing procedures is performed.

Fig. 6. The image showing the wires which contain the data come out of the hole which is placed left side of the oven and these wires are connected to the computers and power supplies.

By using this oven hysteresis also checked by using the cycles of temperature from -20°C to 80°C and again to -20°C. Note that the higher temperature limit is set to the 80°C to prevent damage to the electronics and the connecters.

Compared with hot plate tests circuitry is improved and it is possible to check the package temperature with temperature sensor so these tests are more reliable. The average TCF value is found -130ppm/°K. **Table 3** shows the result of the Design-4 type resonator sensor on Tenney oven. After the calculation according to the Equation 1 the average TCF value is calculated as - 130ppm/°K.

Table 3. Tabulated form of the resonance test results of best performance resonator sensor (the tuning fork double mass together with varying gap structures) is measured using the real time data acquisition from the resonators where resonance frequency is monitored for different temperatures using Tenney temperature oven. (Notice tests are constructed at 5Hz span, 1mV peak voltage and 5 second of integration and settling time).

Temp. (°C)	Res. Freq. (kHz)	Gain (dB)	Q_R
-25	12.887	35.8	103,097
-15	12.872	33.7	93,621
-3	12.862	33.4	171,503
0	12.855	34.1	93,491
20	12.830	34.9	102,642
40	12.814	35.2	170,862
53	12.799	35.8	341,306
60	12.787	36.1	204,599
70	12.767	37.7	340,456
80	12.751	32.8	255,020
90	12.725	36.0	339,349
100	12.705	34.3	203,288
110	12.688	34.7	253,763
120	12.671	37.1	144,820

In the 16-pin dual in line (DIL) metal package, a commercial temperature sensor named TMP36, is also placed for monitoring temperature inside the sensor package and to show there is a relation between the changing temperature and resonator's resonance frequency, PI controller output and the temperature output. The resonator test results of Design-4 for closed loop operation is presented as PI controller output versus temperature graphs prepared by using MATLAB Software. **Fig. 7** shows the test results of resonator Design-4.

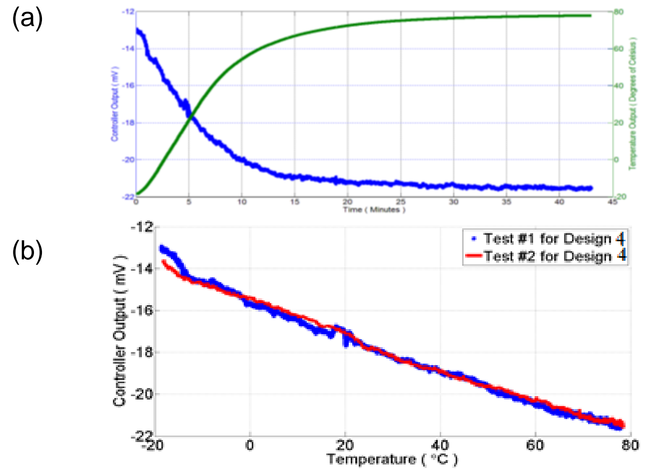

Fig. 7. The test results of resonator package including Design-4 with its readout circuitry put into the Tenney Oven: (a) Design-4 resonator controller output and TMP-36 sensor output changes at the same plot for 45 minutes data collection; (b) Design-4 resonator controller output vs TMP36 sensors output results in the range -20°C to +80°C for different day tests with the same conditions.

The best performance is obtained with the tuning fork double mass together with varying gap structures. **Fig. 8** represents the performance of the resonator Design-4 demonstrated with an ideal line fit. As can be analyzed from the figure the temperature sensitivity of the resonator Design-4 is 0.08 mV/°C; where the temperature coefficient of frequency (TCF) values are measured as -128 ppm/°K in the measurement range in the hot plate and as -114 ppm/°K in the measurement range in the oven.

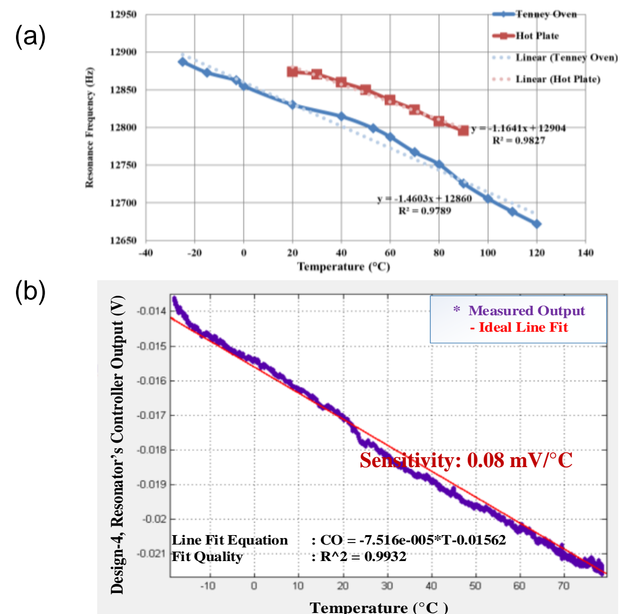

Fig. 8. (a) The resonance frequency versus temperature graph results of the Hot Plate and the Tenney Oven for the tuning fork double mass together with varying gap structures. For these tests the temperature coefficient of frequency (TCF) values are measured as 128 ppm/K in the measurement range in the hot plate and as 114 ppm/K in the measurement range in the oven. (b) The controller output versus temperature graph results of the Tenney Oven for the tuning fork double mass together with varying gap structures. The temperature sensitivity of the resonator Design-4 is 0.08 mV/°C.

The TCF values are found by averaging each two points' TCF value and this was a bit wrong. That is why; a line is fit and found the correct TCF values which can be found in **Fig. 8**. The slope of the hot plate is - 1.1641(Hz/˚C) and the slope of the Tenney oven is - 1.4603(Hz/˚C). At room temperature the resonance frequency of the resonator is determined as 12.830 kHz. When each slope is divided to this resonance frequency and then multiplied with 10^6; the TCF values in ppm/K is obtained. For these tests average TCF value is calculated on hot plate with narrow range as -128 ppm/°K; and the average TCF value is calculated on Tenney with a broader range as -114 ppm/°K. Note that a second or even third order curve fitting would result in a much more precise compensation work. However, since this work is ultimately intended for a real-time compensation practice, and this real-time compensation is intended to be based on a first order fit, the data processing was also conducted using a first order curve fitting.

Minimum detectable temperature change for the resonator packages are collected at 250 Hz for 5 minutes at room temperature (20°C); then these data are processed for collecting the White noise and **Fig. 9**. depicts the Design-4 Allan Variance analysis result. **Table 4** shows the tabulated form of the scale factor, random walk and white noise of the all resonator packages.

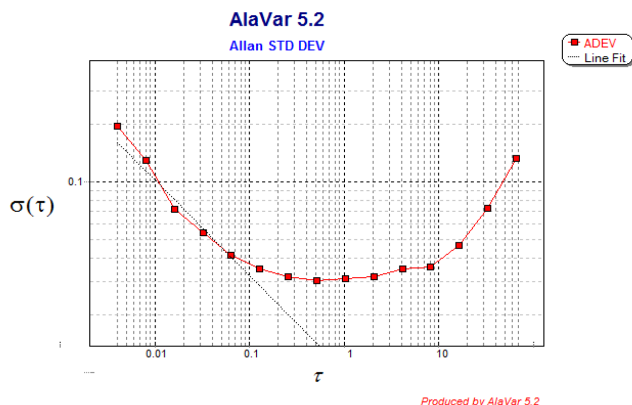

Fig. 9. The sample Alavar output for Design-4; 15 kHz tuning fork varying gap type resonator sensors and this output is given for 75000 data collected from DAQ.

Table 4. Tabulated form of the temperature sensors' scale factor, random walk and white noise values.

Sensor ID	Scale Factor (mV/˚C)	Random Walk (˚C/$\sqrt{Hz}$)	White Noise (˚C/$\sqrt{Hz}$)
Design-1	-3.200	0.00849	12.00e-3
Design-2	-3.217	0.00044	6.14e-4
Design-3	-2.073	0.01181	16.50e-3
Design-4	-0.080	0.01015	14.20e-3

These results show that resonant based MEMS temperature sensor provide a very good sensitivity to be used for compensating the temperature sensitivity of high-performance MEMS sensors such as gyroscopes and accelerometers without complex control electronics.

Results and discussion

Ideally in the literature for any temperature tests range is from -40°C to 85°C and back to -40°C (for mostly industrial application analysis). For all type of resonator packages tests will be done from -20°C to 80°C and back to -20°C which is a suitable range for preferred temperature Oven. Therefore, instead of hot plate, more reliable and repeatable temperature oven is selected for the temperature tests and this way they are significantly improved. It is also experienced that when higher temperatures up to 120°C is reached unfortunately cables and polymer like structures become burned and melted so the range is as previously mentioned from - 20°C to 80°C and back to -20°C.

In this study, the duration of data collections with DAQ varies from 5 minutes to 2 hours and the effect of duration of data collection is not affecting any compensation at all.

To generalize the compensation methods, the data sets taken from each sensor are very significant. For those purposes more than 10 sets of data (for making sure they are repeatable) are collected from each sensor to verify the concept of this study and to improve the reliability of the testing procedures.

Functionality tests are applied to make sure that the resonator package which consists of produced temperature behaved resonator sensor and its circuitry is functional. The circuitry has to be tested block by block; i.e. preamplifier, gain stage, demodulator, low pass filter, modulator and temperature sensor are analyzed, and functionalities are checked. During the tests, in amplitude control due to high noise, a problem is faced and one of the designs is locked another electronic mode which has nearly 35 kHz resonance frequency. To solve this problem a capacitor is added to the 2nd gain stage. Surely nonfunctional dies are omitted to not cause any fault.

In this study, hysteresis in a resonator's controller output data caused by temperature cycles is also analyzed. Notice that for the output to be more accurate, hysteresis has to be removed from the resonator's controller output data. For that purposes heating up and cooling down data are collected with DAQ in the specified temperature range. The two ends of plots, where the temperature stability is high, coincide, but the transient period is not it is most probably because of non-linearity and high settling time of the controller output. **Fig. 10** indicates the comparison of cooling down and heating up characteristics of the MEMS temperature sensors for the different sampling conditions.

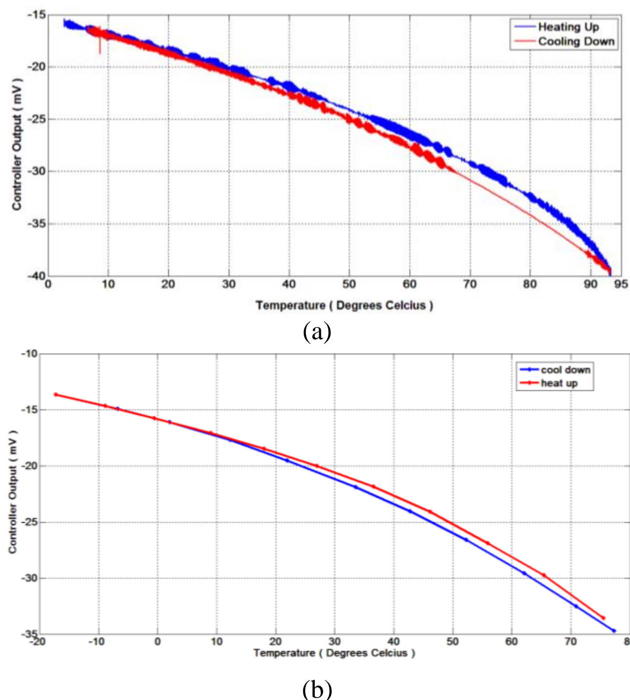

(a)

(b)

Fig. 10. (a) The comparison of heating up and cooling down characteristics of the sampling conditions of 100 Hz 2 hours. (b) The comparison of cooling down and heating up characteristics of the sampling conditions of 250 Hz 5 minutes for each point.

Conclusion

The performance of each sensor is measured using the real time data acquisition from the resonators where resonance frequency and resonator controller outputs are monitored for different temperatures. The best performance is obtained with the tuning fork double mass together with varying gap structures, where the temperature coefficient of frequency (TCF) values are measured as 128 ppm/°K in the measurement range in the hot plate and as 114 ppm/°K in the measurement range in the oven. To sum up, in this study, resonance - based temperature sensors are developed using a wafer level vacuum packaged SOI MEMS process which is normally used to implement various MEMS sensors, including MEMS gyroscopes and accelerometers. Implementing MEMS temperature sensors in such a MEMS process together with sensitive MEMS sensors allows obtaining temperature data, which is very useful for the compensation of a number of parameters of these MEMS sensors for obtaining improved performance. As a future study, these resonance-based MEMS temperature sensors will be used for temperature compensation of MEMS capacitive accelerometer.

Acknowledgements

Authors would like to thank to Dr. M. Mert Torunbalcı and Dr. Said Emre Alper for developing aMEMS process and valuable supports. We also would like to thank Dr. M. Mert Torunbalcı, Orhan Akar and Hasan Doğan Gavcar for their assistance during the fabrication of sensors. Many thanks to Yunus Terzioğlu and Ferhat Yeşil for their unique contributions on the development of readout electronics studies for MEMS resonators.

Author's contributions

T.A. supervised the studies. G.D.A. proposed the study, conceived the design, performed the microfabrication, measurements, developed the simulation technique, and analyzed the results. T.A. and G.D.A. wrote the manuscript. Authors have no competing financial interests.

Keywords

MEMS based resonator, resonance-based temperature sensor, resonance frequency.

Received: 28 September 2019
Revised: 13 December 2019
Accepted: 23 December 2019

References

1. Torunbalci, M. M.; Alper, S. E.; Akın, T.; *IEEE/ASME J. Microelectromechanical Syst.;* **2015**, *24,* 556.
2. Ramm, P.; Lu, J. J. Q.; Taklo, M. M. V. (Ed); Handbook of Wafer Bonding, First Edition; Wiley-VCH Verlag GmbH & Co. KGaA, **2012**.
3. Abdolvand, R.; Bahreyni, B.; Johusa, E.; Lee, Y.; Nabki, F.; *Micromachines*; **2016**, *7,* 160.
4. Dessalegn, H.; Srinivas, T.; 2013 International Conference on Microwave and Photonics; **2013**; pp 1–4.
5. Errando-Herranz, C.; Niklaus, F.; Stemme, G.; Gylfason, K. B.; 2015 Transducers - 2015 18th International Conference on Solid-State Sensors, Actuators and Microsystems (TRANSDUCERS); **2015**; pp 1001.
6. Wu, G.; Xu, D.; Xiong, B.; Wang, Y.; Ma, Y.; *J. Microelectromechanical Syst.;* **2012**, *21,* 1484.
7. Rinaldi, M.; Hui, Y.; Zuniga, C.; Tazzoli, A.; Piazza, G.; IEEE International Frequency Control Symposium Proceedings; **2012**; pp 1–5.
8. Hauptmann, P.; Lucklum, R.; Schroder, J.; IEEE Symposium on Ultrasonics, **2003**; pp 56–65.
9. Nguyen, C. T. C.; IEEE Trans. Ultrason. Ferroelectr. Freq. Control **2007**, *54,* pp 251–270.
10. Hopcroft, M. A.; Agarwal, M.; Park, K. K.; Kim, B.; Jha, C. M.; Candler, R. N.; Yama, G.; Murmann, B.; Kenny, T. W.; 19th IEEE International Conference on Micro Electro Mechanical Systems; **2006**, pp 222–225.
11. Hopcroft, M. A. Temperature-Stabilized Silicon Resonators for Frequency References, Stanford University, **2007**.
12. Melamud, R.; Chandorkar, S. A.; Kim, B.; Lee, H. K.; Salvia, J. C.; Bahl, G.; Hopcroft, M. A.; Kenny, T. W.; *J. Microelectromechanical Syst.;* **2009**, *18,* 1409.
13. Melamud, R.; Kim, B.; Chandorkar, S. A.; Hopcroft, M. A.; Agarwal, M.; Jha, C. M.; Kenny, T. W.; *Appl. Phys. Lett.;* **2007**, *90,* 244107.
14. Kaajakari, V.; VTI Technologies 2011 Joint Conference; **2011**.
15. Dermihan, G.; Resonance-Based MEMS Temperature Sensors for Temperature Compensation of MEMS Capacitive Accelerometer, Middle East Technical University, **2016**.